

Fabrication of Ordered Arrays of Anodic Aluminum Oxide Pores with Interpore Distance Smaller than the Pitch of Nano-pits formed by Ion Beam Etching

Wang CE¹, Tanaka S², Saito K¹, Shimizu T¹ and Shingubara S¹

¹Graduate School of Science and Engineering, Kansai University, Osaka, Japan

²National Institute of Information and Communications Technology (NICT), Japan

*Corresponding author: Wang CE, Graduate School of Science and Engineering, Kansai University, Osaka, Japan, E-mail: wce1979@hotmail.com

Citation: Wang CE, Tanaka S, Saito K, Shimizu T, Shingubara S (2014) Fabrication of an Ordered Anodic Aluminum Oxide Pore Arrays with an Interpore Distance Smaller than the Nano-pits Pitch formed by Ion Beam Etching. *J Mater Sci Nanotechnol* 1(1): S105. doi: 10.15744/2348-9812.1.S105

Received Date: May 27, 2014 **Accepted Date:** July 02, 2014 **Published Date:** July 04, 2014

Abstract

We investigated a method for preparation of ordered nanopore arrays with the interpore distance of 60 nm by guided self-organization of anodic aluminum oxide with a prepatterned array of pits in the starting Al film. An ordered triangular array of 100 nm-pitch pits was formed on Al film by ion beam etching through an electron beam lithography fabricated mask, and then it was used as a guide for formation of anodic aluminum oxide pores. We found it was possible to reduce the interpore distance to $1/\sqrt{3}$ of the pitch of the pits by the appropriate choice of the parameters of ion beam etching and anodization voltage.

Introduction

Anodic aluminum oxide (AAO) has ordered honeycomb structure of pores obtained by self-organization; these pores are perpendicular to the surface and parallel to each other [1-3]. The interpore distance of AAO can be controlled from several tens of nanometers to hundreds of nanometers depending on the anodic voltage and the type of aqueous acid solution used as the electrolyte [4-9]. Moreover, the diameter and the depth of the pores are also controllable by growth conditions, such as anodic voltage and duration of anodization, respectively. The regularity of AAO pore arrangement is one of the important issues for applications such as ultra-high density patterned media using magnetic nanowire arrays [10-16], and the patterning of surfaces for sensors [17-19], optically active surfaces [20,21], and for substrates for controlled living cell cultures [22-24], and AAO nanopore arrays are considered as the suitable structure for preparation of nanowire and nanodot of various materials [25], such as magnetic and semiconductor materials. However, it is known that the ordered AAO pore arrays can be obtained by several appropriate growth conditions [26], and the inter-pore distances of ordered AAO pore arrays are limited. Moreover, preparation of fine pitch arrays is getting more difficult, especially below 100 nm.

Nanoimprinting is an effective method to form perfectly ordered AAO pore arrays [4,27-29], which utilizes a combination of top-down and bottom-up techniques. The periodically pitted Al surface was prepared prior to anodization using a hard mold or dry etching with hole-patterned mask [30]. Then, the nanopores start to grow one-to-one at the pit positions. However, also with this method it is difficult to obtain ordered pore arrays with the interpore distance of a few tens of nm due to the size limitation of EBL (electron beam lithography) and dry etching technology.

A reduction in AAO interpore distance to 300 nm by a factor of $1/\sqrt{3}$ was achieved by Choi et al. [31,32] by nanoimprinting with mold that had a pitch of 500 nm. Recently, our group succeeded in preparation of 115 nm pitch AAO pore arrays using a guided self-organization method, and nanoimprinting process with a SiC mold with a pitch of 200 nm. In this study, we tried to prepare AAO on Si substrate with an interpore distance of 60 nm using a guided self-organization method.

Experiments

The experimental procedure is described schematically in Figure 1(a)-(f). At first, 500 nm thick Al film was deposited on treated Si substrate (Si was treated with HF solution) by sputtering using Al target (99.999%, High Purity Materials KONJUNDO CHEMICAL LABORATORY CO.LTD, JAPAN) as shown in Figure 1(a). The surface roughness of Al film is very important for pre patterning method, and the root mean square surface roughness (RMS) was less than 10 nm, which was measured by atomic force microscopy (AFM) (1 μm \times 1 μm scan). Then, about 100 nm thickness resist film was fabricated by spincoating method (300 rpm 5 sec, 2000 rpm 180 sec) using ZEP520A resist (use Anisol diluted into 2:3) as shown in Figure 1(b), the pre-bake was carried

out on 180 °C hot plate at 180 sec after spincoating. Subsequently, the triangular lattice of pits with a pitch of 100 nm was prepared by EBL on sputtered Al film on Si substrate as shown in Figure 1(c). 75 kV acceleration voltage electron beam selectively etches off regions of the positive resist from the surface (ELIONIX ELS-7700, JAPAN). Ion beam etching (IBE) was carried out at 23 °C with 180 sec using ZED-N50 developing solution. Then, using pits pattern as a mask for Ar (Figure 1(d)), IBE was carried out for different duration times under the conditions of 150 V beam voltage and 700 V accelerator voltage in a chamber (RIB-E, TYD, JAPAN) at 2.5×10^{-2} Pa. We then transferred the triangular lattice pattern to the Al surface as shown in Figure 1(e). For Ar IBE, acceleration voltage was kept constant at 700 V, and etching time was changed from 5 min to 10 min. After that, the EBL resist mask was completely removed from Al surface by selective etching with 10 min in acetone. The Al surface of 10 min IBE sample was observed by scanning electron and atomic force microscopy (AFM and SEM), Figure 2(a)-(b), respectively. Figure 2(c) shows an AFM line scan extracted from Figure 2(b). According to the AFM profile we can know that the interpore distance was approximately 100 nm, the depth was 50 nm, and the arrangement of pits was perfectly ordered as triangular lattice without any defects and dislocations. Thus, the periodically prepatterned Al surface was obtained. Then, prepatterned Al surface was anodized at various voltages between 24 to 30 V in 0.3 M sulfuric acid electrolytes as shown in Figure 1(f). Figure 1(g) and (h) shows the surface of the Figures (e) and (f), respectively. The pits having an ordered triangular array of nanopores with a pitch of 100 nm on Al surface shows in Figure 1(g), and the Al is anodized after prepattern, the small dots were formed at the center of each triangle of the initial pits, then $1/\sqrt{3}$ reduction of interpore distance is achieved at an adequate anodic voltage. The surface morphology of Al and AAO pore arrays were observed by scanning electron microscope (SEM) and AFM. The regularity of AAO pores was quantitatively evaluated by the fast Fourier transforms (FFT) of the SEM images.

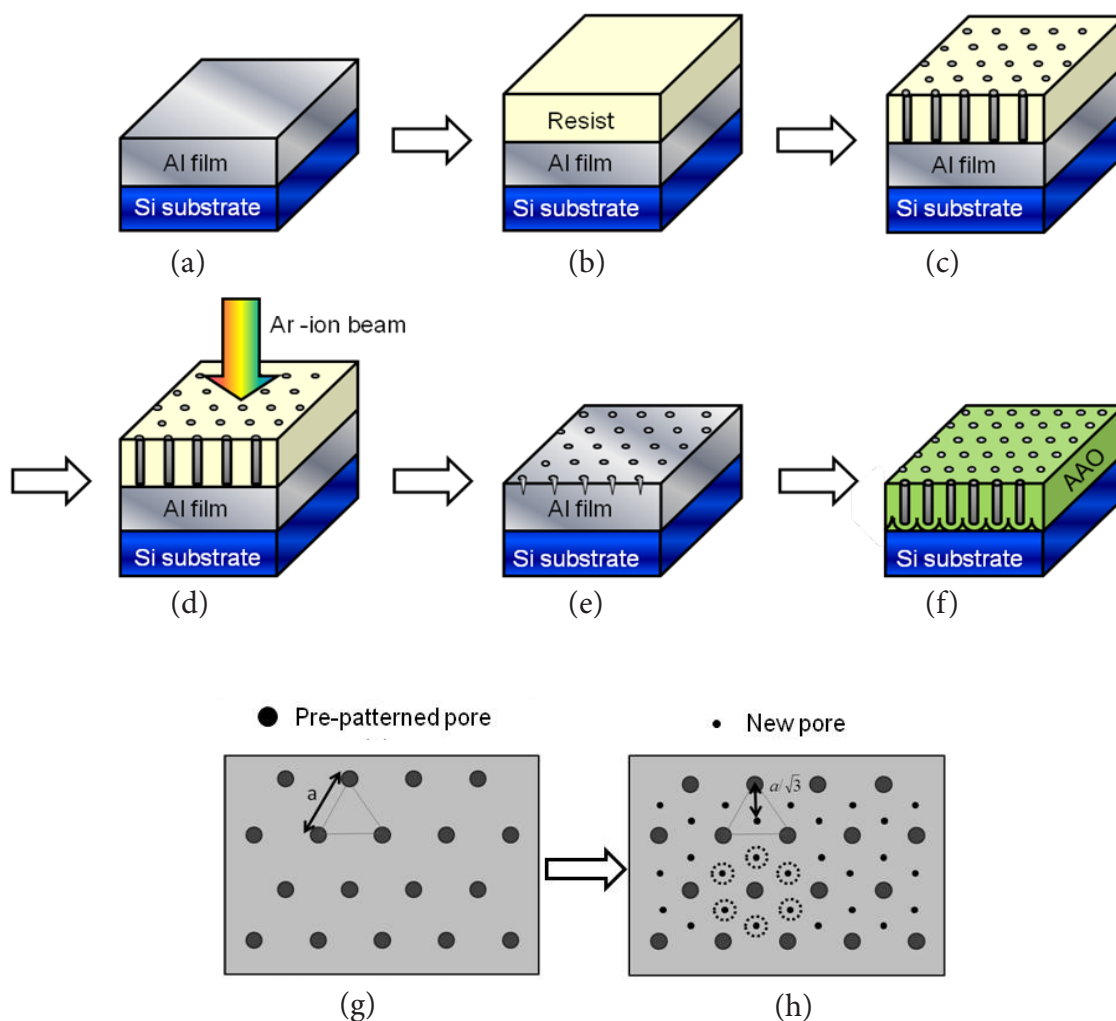


Figure 1: Schematics of the sample preparation (a) Al film is sputtered on Si substrate. (b) Resist film is fabricated using spin-coating method. (c) The periodically holes is fabricated in resist film by electron beam lithography. (d) Formation of pits on Al film by IBE. (e) Removal the EBL resist mask. (f) Anodic oxidation of Al. (g) The top-view of (e), dots indicate indentations having an order triangular array. (h) The top-view of (f), the smaller dots indicate position of new pores formed by anodization.

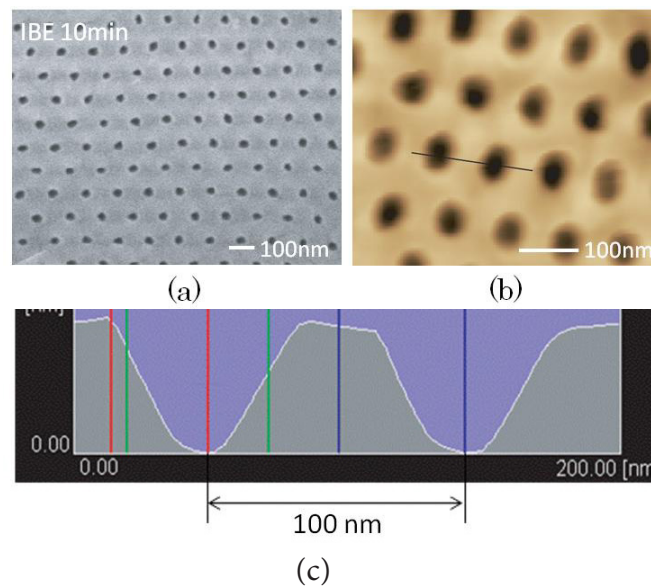


Figure 2: SEM and AFM measurements of the ordered nanopore arrays after pre patterning on Al surface. (a) Nanopores of pre patterned Al surface were observed by SEM after ion beam etching at 10min, the inter pore distance of nanopore was approximately 100nm. (b) Nanopores of pre patterned Al surface were observed by AFM. (c) Line scan of AFM height image shown in (b).

Results and Discussions

Figure 3 shows top-view SEM images of the AAO pore arrays using patterned Al films, which was anodized at various voltages from 24 to 30 V. It can be observed that the inter pore distance between the larger AAO pores indicated with black circles was 100 nm, which corresponds to the pitch of the IBE mask. Therefore, these pores were grown at the pre patterned positions on the Al surface. The smaller pores indicated with dashed circles were newly created pores located at the center of hexagon of pre patterned pores, which worked as the guide to determine a position of nucleation sites of new pores. The anodic voltage dependence of pore arrangement is shown in Figure 3(a)-(c). Although the arrangement of the new AAO pores was not a perfect triangular lattice, we found that 28 V is an appropriate voltage to realize the reduction of the pitch for the array pre patterned with 100 nm pitch in these conditions. Some pre patterned AAO pores are elongated with two-fold depression at a single location, as indicated for example by the arrows in Figure 3(a) and (c). It seems that the dislocation and defect of the triangular AAO pore arrays are caused by the oversized pits for the guided self-organization, and the size and depth of pits would be important.

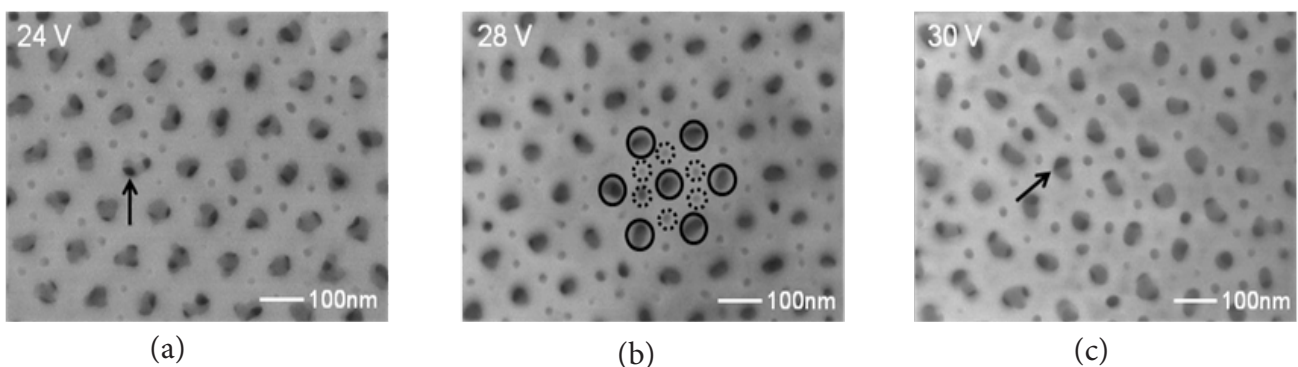


Figure 3: SEM image of the surface of AAO after anodic oxidation of aluminum for various anodization voltages. (a) 24V anodic voltage. (b) 28V anodic voltage. (c) 30V anodic voltage.

Figure 4(a)-(c) shows top-view SEM images of AAO pore arrays using guided self-organization method with different duration of IBE for pre patterning. We analyzed the SEM images by two-dimensional FFT to evaluate the IBE duration dependence of the nanohole regularity as shown in Figure 4(d)-(f). The triangular arrays of spots were clearly observed in 7.5 and 10 min of IBE etching samples while only fuzzy spots were observed in the 5 min sample. The cross section of the FFT intensity distribution along the red line is shown in the Figure 4(g)-(i). The regularity of the nanohole arrangement is well represented by the intensity of order spots (indicated with arrows in Figure 4(h) and (i)). Hence, we chose a spatial order parameter, I/W (the first spots intensity I divided by its full width at half maximum width (FWHM) W) [33]. In the FFT cross sections, two series of peaks appear at increasing distances from the center (first spot and second spot are shown in Figure 4(h) and Figure 4(i), respectively). The periodic

function of structure such as nanohole arrays in real space corresponds to the reciprocal distance of ordered spot in FFT image. Therefore, the first ordered spots in Figure 4 (i) correspond to the original prepatterned lattice (~ 100 nm pitch), and the second ordered spots are secondary lattice formed by anodization (~ 60 nm pitch), respectively. The regularity ratio I/W of the prepatterned lattice peak increases from Figure 4(g) to Figure 4(i), as expected, since longer IBE patterning time means better defined starting pattern. However, the peak arising at higher spatial frequency (i.e. lower pitch) due to anodization, Table 1 shows regularity as a function of the IBE duration; has the highest regularity ratio about 7.3 for the intermediate case of Figure 4(h) 7.5 min IBE, and it seems that the pits of 5 min IBE was not enough for the guide of new pores. These results suggested that 7.5 min IBE was the appropriate condition for guided self-organization of interpore distance of 60 nm, while the 10 min IBE caused over-etching.

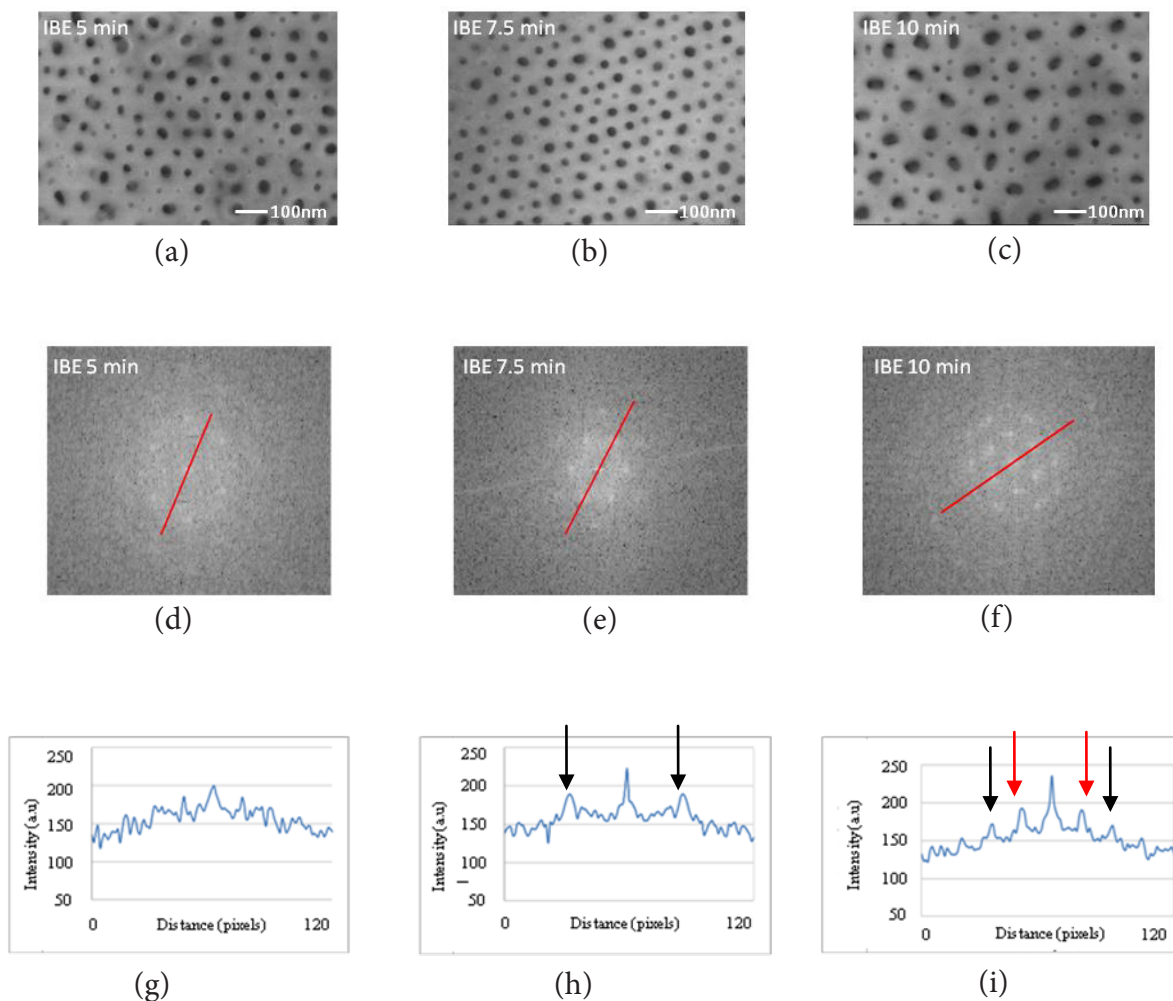


Figure 4: SEM micrographs of the surface of AAO after anodic oxidation of aluminum at 28V for various ion beam etching times. (a)-(c) The top-view SEM images of surface of the AAO membrane just after anodic oxidation at 28V with 5min, 7.5min, 10min IBE times. (d)-(f) Two-dimensional FFT images for the nanopore arrangements shown in Figure 4 (a)-(c). (g)-(i) are cross-section of the FFT intensity distribution along the red line in Figure 4 (d)-(f). The red and black arrows in Figure (d)-(f) indicate first- and second-ordered spots of nanohole arrays.

IBE duration [min]	5	7.5	10
Regularity (I/W)	2.4 ± 0.2	7.3 ± 0.2	4.1 ± 0.2

Table 1: Ion beam etching duration dependence of nanohole regularity

Conclusions

The ordered nanopore arrays with the interpore distance of 60 nm on Si substrate were successfully prepared using 100 nm pitch masks of prepatterned Al films with IBE and guided self-organizing of AAO. It turned out that there was an appropriate IBE condition and anodization voltage for realizing ordered AAO nanopore arrays in this method. This method allows further reduction of AAO interpore distance, and it would be possible to realize triangular pore arrays with smaller interpore distance beyond the size limitation of the lithographic technique [34-37].

Acknowledgement

This work is partially supported by the Grant – in – Aid for Scientific Research 20241027 of JSPS, and Strategic Project to Support the Formation of Research Bases at Private Universities: Matching Fund Subsidy from MEXT (Ministry of Education, Culture, Sports, Science and Technology).

References

1. Masuda H, Fukuda K (1995) Ordered metal nanohole arrays made by a two-step replication of honeycomb structures of anodic alumina. *Science* 268: 1466-8.
2. Keller F, Hunter MS, Robinson DL (1953) Structural Features of Oxide Coatings on Aluminum. *J Electrochem Soc* 100: 411-9.
3. O'Sullivan JB, Wood GC (1970) The Morphology and Mechanism of Formation of Porous Anodic Films on Aluminium. *Proc R Soc London Ser A* 317: 511-43.
4. Masuda H, Satoh M (1996) Fabrication of Gold Nanodot Array Using Anodic Porous Alumina as an Evaporation Mask. *Jpn J Appl Phys* 35: L 126.
5. Masuda H, Tanaka H, Baba N (1993) Preparation of Microporous Gold Films by Two-Step Replicating Process Using Anodic Alumina as Template. *Bull Chem Soc Jpn* 66: 305-11.
6. Masuda H, Hasegawa F, Ono S (1997) Self Ordering of Cell Arrangement of Anodic Porous Alumina Formed in Sulfuric Acid Solution. *J Electrochem Soc* 144: L 127-30.
7. Masuda H, Yada K, Osaka A (1998) Self-Ordering of Cell Configuration of Anodic Porous Alumina with Large-Size Pores in Phosphoric Acid Solution. *Jpn J Appl Phys* 37: L 1340.
8. Shingubara S, Okino O, Sayama Y, Sakaue H, Takahagi T (1997) Ordered Two-Dimensional Nanowire Array Formation Using Self-Organized Nanoholes of Anodically Oxidized Aluminum. *Jpn J Appl Phys* 36: 7791.
9. Jessensky O, Muller F, Grosele U (1998) Self-organized formation of hexagonal pore arrays in anodic alumina. *Appl Phys Lett* 72: 1173.
10. Stephen YC (1997) Patterned magnetic nanostructures and quantized magnetic disks. *Proc IEEE* 85: 652-71.
11. Niklasson GA, Bobbert PA, Craighead HG (1999) Optical properties of square lattices of gold nanoparticles. *Nanostruct Mater* 12: 725-30.
12. Li Y, Meng GW, Zhang LD (2000) Ordered semiconductor ZnO nanowire arrays and their photoluminescence properties. *Appl Phys Lett* 76: 2011
13. Wernsdorfer W, Doudin B, Maillly D, Hasselbach K, Benoit A, et al. (1996) Nucleation of Magnetization Reversal in Individual Nanosized Nickel Wires. *Phys Rev Lett* 77: 1873-76.
14. Piraux L, George JM, Despres JF, Leroy C, Ferain E, et al. (1994) Giant magnetoresistance in magnetic multilayered nanowires. *Appl Phys Lett* 65: 2484.
15. Garcia JM, Asenjo A, Velázquez J, Garcia D, Vázquez M, et al. (1999) Magnetic behavior of an array of cobalt nanowires. *J Appl Phys* 85: 5480.
16. Shingubara S, Morimoto K, Nagayanagi M, Shimizu T, Yaegashi O, et al. (2004) Aspect ratio dependence of hysteresis property of high density Co wire array buried in porous alumina template. *J Magn. Magn Mater* 272-276: 1598-9.
17. Takhistov P (2004) Electrochemical synthesis and impedance characterization of nano-patterned biosensor substrate. *Biosens Bioelectron* 19: 1445-56.
18. Salerno M, Patra N, Diaspro A (2011) Anodization of aluminium coated atomic force microscopy microcantilevers for conversion of the coating into nanoporous alumina. *Microelectronic Engineering* 88: 2383-5.
19. Lee D, Shin N, Lee K, Jeon S (2009) Microcantilevers with nanowells as moisture sensors. *Sensors and Actuators B* 137: 561-5.
20. Choi J, Schilling J, Nielsch K, Hillebrand R, Reiche M, et al. (2002) Large-area porous alumina photonic crystals via imprint method. *Mat Res Soc Symp Proc* 722.
21. Das G, Patra N, Gopalakrishnan A, Zaccaria RP, Toma A, et al. (2012) Fabrication of large-area ordered and reproducible nanostructures for SERS biosensor application. *Analyst* 137: 1785-92.
22. Poinern, Shackleton R, Mamun SI (2011) Significance of novel bioinorganic anodic aluminum oxide nanoscaffolds for promoting cellular response. *Nanotechnology, Science and Applications* 4: 11-24.
23. Salerno M, Giacomelli L, Larosa C (2011) Biomaterials for the programming of cell growth in oral tissues: The possible role of APA. *Bioinformation* 5: 291-3.
24. Toccafondi C, Thorat S, La Rocca R, Scarpellini A, Salerno M, et al. (2014) Multifunctional substrates of thin porous alumina for cell biosensors. *J Mater Sci Mater Med*: Epub ahead of print.
25. Shingubara S, Murakami Y, Morimoto K, Takahagi T (2003) Formation of aluminum nanodot array by combination of nanoindentation and anodic oxidation of aluminum. *Surface Science* 532-5: 317-23.
26. Shingubara S (2003) Fabrication of Nanomaterials Using Porous Alumina Templates. *Journal of Nanoparticle Research* 5: 17-30.
27. Masuda H, Yamada H, Satoh M, Asoh H (1997) Highly ordered nanochannel-array architecture in anodic alumina. *Appl Phys Lett* 71: 2770.
28. Shingubara S, Maruo S, Yamashita T, Nakao M, Shimizu T (2010) Reduction of pitch of nanohole array by self-organizing anodic oxidation after nanoimprinting. *Microelectronic Engineering* 87: 1451-4.
29. Chen B, Lu K, Tian Z (2010) Novel patterns by focused ion beam guided anodization. *Langmuir* 27: 800-8.
30. Huang Z, Zhang X, Reiche M, Liu L, Lee W, et al. (2008) Extended arrays of vertically aligned sub-10 nm diameter [100] Si nanowires by metal-assisted chemical etching. *Nano Lett* 8: 3046-51.
31. Choi J, Nielsch K, Reiche M, Wehrspohn RB, Gosele U (2003) Fabrication of monodomain alumina pore arrays with an interpore distance smaller than the lattice constant of the imprint stamp. *J Vac Sci Technol B* 21: 763-6.
32. Choi J, Wehrspohn RB, Gosele U (2005) Mechanism of guided self-organization producing quasi-monodomain porous alumina. *Electrochim Acta* 50: 2591-5.
33. Toccafondi C, Stępniewski WJ, Leoncini M, Salerno M (2014) Advanced morphological analysis of patterns of thin anodic porous alumina. *Mater Characterization* 94: 26-36.
34. Maria Chong AS, Tan LK, Deng J, Gao H (2007) Soft Imprinting: Creating Highly Ordered Porous Anodic Alumina Templates on Substrates for Nanofabrication. *Adv Funct Mater* 17: 1629.
35. Sun Z, Kim HK (2002) Growth of ordered, single-domain, alumina nanopore arrays with holographically patterned aluminum films. *Appl Phys Lett* 81: 3458.
36. Oshima H, Kikuchi H, Nakao H, Itoh K, Kamimura T, et al. (2007) Detecting dynamic signals of ideally ordered nanohole patterned disk media fabricated using nanoimprint lithography. *Appl Phys Lett* 91: 22508.
37. Chou SY, Krauss PR, Renstrom PJ (1995) Imprint of sub 25 nm vias and trenches in polymers. *Appl Phys Lett* 67: 3114.

Submit your next manuscript to Annex Publishers and benefit from:

- ▶ Easy online submission process
- ▶ Rapid peer review process
- ▶ Online article availability soon after acceptance for Publication
- ▶ Open access: articles available free online
- ▶ More accessibility of the articles to the readers/researchers within the field
- ▶ Better discount on subsequent article submission

Submit your manuscript at
<http://www.annexpublishers.com/paper-submission.php>